

## Photoelectron studies of the densities of states in the gallium chalcogenides

F. R. Shepherd\* and P. M. Williams†

*Department of Chemical Engineering and Chemical Technology, Imperial College, London, England*

(Received 3 June 1975)

Photoelectron energy distributions for the layered semiconductors GaSe and GaS are reported using Ne<sub>I</sub>, He<sub>I</sub>, He<sub>II</sub>, and Mg K $\alpha$  photons. The deep-lying chalcogen *s* bands and the gallium 3*d* core levels have been located, and considerable structure resolved in the main *p*-like bonding band for both materials. The empirically determined density of states have been compared with that determined from a pseudopotential-energy-band scheme, and good agreement is seen for features in the energy distributions recorded at high photon energy (He<sub>II</sub> or Mg K $\alpha$ ). In addition to this information on the occupied energy bands, the secondary electron background observed in both He and Ne<sub>I</sub> energy distributions is shown to exhibit pronounced structure characteristic of the one-electron conduction-band density of states, where again, close correlations are observed with the calculated-energy-band scheme.

### I. INTRODUCTION

The gallium chalcogenides GaSe and GaS are layered semiconductors characterized by considerable anisotropy in their physical properties. Their somewhat unexpected adoption of a lamellar structure results from the formation of strong Ga-Ga bonds between superimposed sheets of gallium atoms; these sheets are then "sandwiched" by sheets of chalcogen atoms resulting in a fourfold S-Ga-Ga-S layer as in Fig. 1 (with similar for the selenide). The local (Ga<sub>2</sub>)S<sub>2</sub> trigonal prism coordination unit may thus be considered in some respects analogous to that in MoS<sub>2</sub>. Various stacking sequences of these fourfold layers are found as discussed by Basinski *et al.*,<sup>1</sup> the hexagonal  $\beta$  phase being commonest in crystals of GaS, and the mixed hexagonal  $\epsilon$  and rhombohedral  $\gamma$  phases in GaSe.

The distinct difference in intra- and interlayer bonding is reflected in the large degree of anisotropy in the optical and transport properties of these materials, while the pairing of metal atoms in the structure results in filled bands and semiconducting behavior. Thus optical studies<sup>2</sup> reveal strong excitonic absorption associated with a direct gap (at  $\Gamma$ ) of 3.05 eV for GaS and 2.17 eV for GaSe, as well as a weaker edge associated with an indirect gap of 2.59 eV for GaS and 2.12 eV for GaSe. The energy-band structure of GaSe has been calculated in the single-layer approximation using a tight-binding method.<sup>3</sup> More recently, a full three-dimensional calculation of the energy bands for  $\beta$ -GaSe has been made using an empirical-pseudopotential approach,<sup>4,5</sup> fitted to the optically determined parameters. In general, the valence bands predicted by these two methods are similar, but considerable differences appear in the predicted conduction bands, where the tight-binding approach may be thought to give a less accurate description.

Photoelectron spectroscopy using ultraviolet

(UPS) or x-ray photons (XPS) is becoming increasingly widely recognized as a very direct probe of valence-band densities of states in solids, and early XPS measurements<sup>6</sup> on GaSe showed some correlations with the single-layer band-structure calculations. More recent XPS data using monochromatized radiation<sup>7</sup> are in good agreement with the measurements in the present paper. Low-energy photoemission studies using synchrotron radiation in the energy range 14.6–24.1 eV have been reported<sup>8</sup> with an energy resolution of about 0.2–0.3 eV. These results show some agreement with the predicted bands, although the authors pointed out a discrepancy between observed and calculated bandwidths. However, accurate estimates of the latter are complicated by contributions to the spectra from inelastic and secondary electrons at these photon energies. There is clearly a need, therefore, for further measurements at higher resolution over a wider range of photon energies before a conclusive comparison with the calculated-band schemes can be made. This paper reports photoemission studies of both GaSe and GaS at photon energies between 16.8 and 1253.6 eV, recorded under ultra-high-vacuum conditions at high resolution ( $\lesssim 0.1$  eV).

### II. EXPERIMENTAL

The crystals of GaSe and GaS grown by Bridgman techniques and kindly donated by F. Levy (EPF, Lausanne) were in the form of specular disks, about 1 cm diameter and 2 mm thick. After cleavage in an ancillary vacuum chamber of the electron spectrometer (Merris Vacuum Generators, Ltd., model ESCA 3) at a pressure of  $5 \times 10^{-8}$  Torr for GaSe and  $8 \times 10^{-10}$  Torr for GaS, the samples were transferred to the analyzer chamber where the base pressure was in the low  $10^{-10}$  Torr range. Spectra were recorded using a hemispherical analyzer system fitted with a windowless He discharge lamp and an x-ray source with a twin Al-

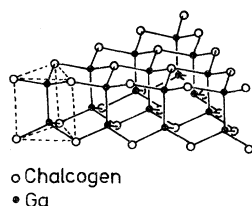


FIG. 1. Single layer of the GaSe structure showing Ga-Ga bonded sheets and the local trigonal prism coordination unit.

Mg anode. With either type of source operating the pressure remained within the  $10^{-10}$  Torr range while spectra were recorded. Digital data acquisition was employed using a computer based signal averaging system directly interfaced to the analyzer. Typical data-acquisition times ranged from 20 min for the UPS spectra to 4 h for the x-ray valence-band measurements. All spectra were recorded at room temperature and unless otherwise stated in the text raw unsmoothed data are presented in all the figures.

### III. RESULTS

#### A. GaSe

Spectra recorded for GaSe using Ne I ( $\hbar\omega=16.8$  eV), He I ( $\hbar\omega=21.2$  eV), He II ( $\hbar\omega=40.8$  eV), and Mg  $K\alpha$  x radiation ( $\hbar\omega=1253.6$  eV) are shown in Fig. 2. The zero of binding energy for all spectra is taken as the valence-band edge  $E_{vb}$ ; the instrumental Fermi level  $E_F$  fixed with reference to the sharp  $d$ -band threshold of Ni under similar experimental conditions is also shown. In all the spectra in Fig. 2 the photoemission threshold at  $E_{vb}$  occurs approximately 0.9 eV below  $E_F$ , consistent with semiconducting behavior as discussed below (the samples were in good electrical contact with the specimen holder). Considerable structure is then observed for each photon energy, but within the region  $E_{vb}-9$  eV, six bands (denoted by  $a$ ,  $b$ ,  $c$ ,  $d$ ,  $e$ , and  $f$  in Fig. 2) are observed for Ne I, He I, and He II. Although changes occur in the relative weighting of these bands, their energy positions remain approximately constant (to within 0.1 eV) while the photon energy is varied when due allowance is made for differences in background between spectra. At the Mg  $K\alpha$ -x-ray energy bands  $a$ ,  $b$ ,  $c$ , and  $d$  are not resolved as a result of the greater exciting linewidth of the radiation ( $\sim 0.8$  eV); band  $e$ , however, appears as a shoulder, while band  $f$  is partly obscured by the pair of  $\alpha_3\alpha_4$  satellite peaks from the Ga 3 $d$  core level. The pair of peaks between 9 and 13 eV in the He II spectrum apparently have no counterparts in any

of the other spectra; both are resolved as a doublet with a splitting of 0.35 eV, and arise from excitation of the Ga 3 $d$  core states by photons at energies of 51.1 and 48.4 eV, respectively, (He II $\gamma$  and He II $\beta$ ). The Ga 3 $d$  core level may also be excited with reduced intensity by He II photons (40.8 eV), giving rise to the weak overlapping structure immediately above the valence-band edge in the He I spectrum in Fig. 2. These overlap effects between spectra excited by photons of different energies necessarily occur when using an unfiltered windowless source as in the present investigation; however, as a result of the relative intensity ratios in the output from the discharge lamp (He I:He II:He II $\beta$ :He II $\gamma$  is approximately 100:25:3:1), an unambiguous interpretation of all structures may usually be given. The exact ratios in any particular experiment depend critically on the lamp operating pressure and the proportion of higher-energy photons being enhanced by lower operating pressures. Figure 3 reproduces the Ga 3 $d$  core level spectra excited by photons at

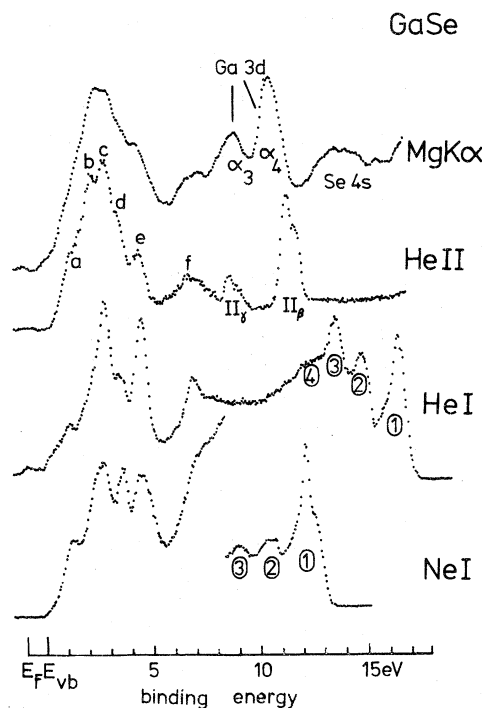


FIG. 2. Photoelectron energy distributions recorded for GaSe cleaved at  $5 \times 10^{-8}$  Torr using Ne I, He I, He II, and Mg  $K\alpha$  photons. Peaks  $a$ ,  $b$ ,  $c$ ,  $d$ ,  $e$ , and  $f$  derive from the  $p$ -like valence electrons; 2, 3, and 4 arise from secondary electron emission out of lowest conduction bands. Extra structure at Mg  $K\alpha$  results from  $\alpha_3\alpha_4$  satellites from the Ga 3 $d$  level, and from the Se 4 $s$  band. In the He II spectrum peaks between 8 and 13 eV below  $E_{vb}$  are Ga 3 $d$  excited by He II $\gamma$  and He II $\beta$ , respectively.

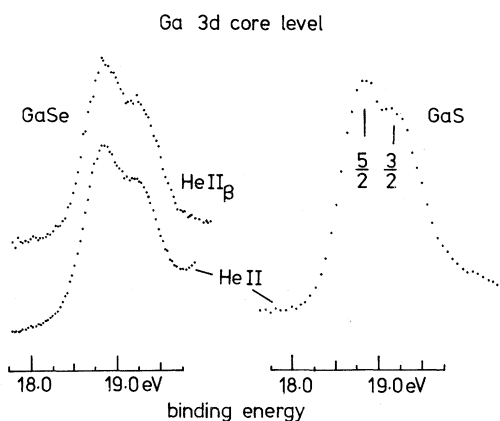


FIG. 3. Expanded trace for Ga 3d core level from: (i) GaSe (He II and He II<sub>β</sub> photons), and (ii) GaS (He II photons), showing the spin-orbit splitting close to 0.4 eV.

40.8 and 48.4 eV for comparison with that excited from GaS at 40.8 eV.

Again with reference to Fig. 2 a broad band (~2 eV wide) is observed with Mg K $\alpha$  radiation at around 15 eV below  $E_{vb}$ ; this has no counterpart in the He II spectrum (and would be obscured by secondary electrons if present in the He I and Ne I spectra). As discussed below, we interpret this band as arising from the excitation of the Se 4s electrons; these states are absent in the He II spectrum as a result of the very low cross section for excitation of s states at uv energies.

Close to the work-function cutoff at He I and Ne I in Fig. 2, considerable structure is observed in the secondary electron background. This structure does not remain constant in binding energy  $E'$  with respect to  $E_{vb}$  when changing photon energy from He I to Ne I. However, when plotted against

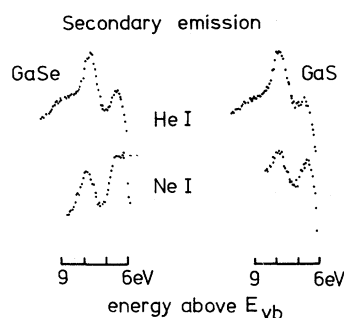


FIG. 4. Secondary electron emission structure for GaSe and GaS from Ne I and He I excited spectra replotted according to kinetic energy above  $E_{vb}$ . Peaks 2 and 3 are constant in energy above  $E_{vb}$  as the photon energy is varied.

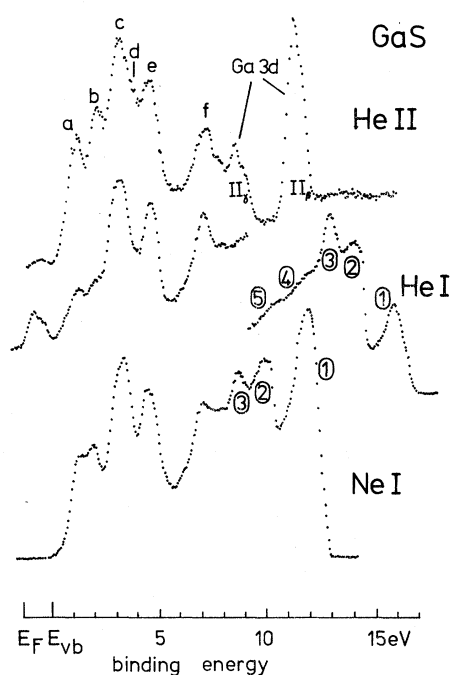


FIG. 5. Photoelectron energy distributions recorded for GaS cleaved at  $8 \times 10^{-10}$  Torr using Ne I, He I, and He II. Peaks a, b, c, d, e, and f as for GaSe, except that d is now only resolved as a shoulder on c. Structure above  $E_{vb}$  in the He I spectrum is due to excitation of Ga 3d by the He II photons.

measured kinetic energy above the band edge (i.e.,  $\hbar\omega - E'$ ) as in Fig. 4, the features in the He I and Ne I spectra are seen to superimpose. The four peaks denoted by 1, 2, 3, and 4 in Fig. 2 may thus be interpreted in terms of secondary electron emission. Note that peak 1 derives from secondary emission from the "cage" surrounding the sample which is normally maintained at sample potential so that both secondary emission and photoemission take place in field-free space. Secondary electrons excited from this cage, therefore, overlap true secondary peaks owing to the sample. However, the application of a small bias voltage between sample and cage moves the sample secondary in energy relative to those from the cage enabling the true contributions from the former together with its vacuum level cutoff (arrowed) to be unambiguously determined. Secondary spectra for GaS are also reproduced in Fig. 4 again with measured energy above  $E_{vb}$  as the abscissa. Two strong secondary emission peaks (2 and 3) are seen for both GaS and GaSe at similar energies relative to the vacuum level. A weaker third peak (4) seen in He I for both materials is obscured in

the Ne I spectra by band *f*. A further peak (5) is present in the He I spectrum of GaS.

### B. GaS

Figure 5 reproduces spectra for GaS cleaved in ultrahigh vacuum for photon energies Ne I, He I, and He II. These spectra closely resemble the spectra of GaSe and again the photoemission threshold  $E_{vb}$  at 1.4 eV below  $E_F$  is consistent with semiconducting properties. The band appearing above the band edge in the He I spectrum arises from excitation of the Ga 3*d* core level by He II photons; its intensity relative to the remaining structure is much greater than that of its counterpart in GaSe (Fig. 2) as a result of the slightly lower operating pressure of the discharge lamp during the GaS experiments. Excitation of this core level by He II<sub>β</sub> and He II<sub>γ</sub> photons is also observed as in GaSe, the He II excited core level being reproduced for comparison in Fig. 3.

As with GaSe six bands denoted by *a* to *f* are common to the spectra at all three photon energies (although band *d* is barely resolved as a weak shoulder on band *c*), and once more some change in weighting of structure with variation in photon energy is observed particularly between He I and He II. Angular effects are also found to be significant especially at low-photon energies, as is seen from the spectra in Fig. 6 recorded using He I radiation. Although independent control of azimuthal and polar angles is not possible with the present analyzer geometry, the spectra in Fig. 6 for different orientations of the crystal show that, whereas peaks *a*, *c*, *e*, and *f* are relatively insensitive to angular changes, peaks *b* and *d* vary considerably both in energy and in relative inten-

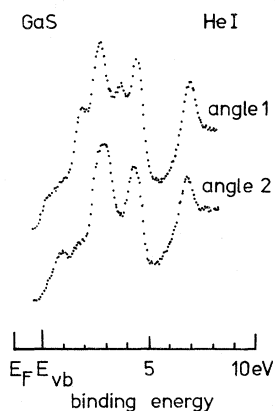


FIG. 6. He I spectra for GaS recorded for two different orientations of crystal relative to analyzer. Peaks *b* and *d* exhibit greatest changes with angle.



FIG. 7. Comparison of the He II energy distributions for GaSe and GaS. Note the shift of bands *c* to *f* to higher binding energy in the sulphide with consequent increase in total bandwidth. Peaks *e* and *f* maintain constant separation for both materials.

sity as is discussed below.

Bands *c*, *d*, *e*, and *f* are similar in relative weighting and position in the spectra from GaS and GaSe (particularly at the He II photon energy), but bands *a* and *b* appear more widely separated from the rest in the sulphide; the over-all bandwidth in GaS is thus greater than in GaSe as is readily seen in the comparison of their He II spectra in Fig. 7. Secondary electron structure is found in both the He I and Ne I spectra of GaS as pointed out above; this structure is replotted as outlined above in Fig. 4. The binding energies of all the photoemission peaks, together with the kinetic energies above  $E_{vb}$  of the secondary emission structure for both GaS and GaSe are tabulated in Table I.

## IV. DISCUSSION

Before considering in detail the origins of the various bands in the photoemission spectra, we will first make the following general comments concerning the observations.

### A. Crystal structure

No attempt was made in the present investigation to establish the three-dimensional stacking sequences in either the GaS or the GaSe crystals. The mean free paths of the photoelectrons at these uv photon energies are short ( $\sim 10 \text{ \AA}$ ) and the measurements, therefore, sense only the uppermost two or three layers. Under these circumstances, bulk x-ray crystallographic deter-

TABLE I. Binding energies of principal features in the photoemission energy distributions of GaSe and GaS, with respect to the valence-band edge  $E_{vb}$ . Possible assignments of bands from Ref. 5 given in terms of their representations at  $\Gamma$ .

Material	Chalcogen $p$ band				Ga-Ga bands		Chalcogen $s$ band	Ga $3d$		
	$E_F - E_{vb}$	$a$	$b$	$c$	$d$	$e$ (antibonding)		$f$ (bonding)	$3d_{5/2}$	$3d_{3/2}$
GaSe	0.9	1.0	2.0	2.6	3.1	4.0	6.4	14.0	18.2	18.6
GaSe	1.4	1.1	2.0	3.0	(3, 5) <sup>a</sup>	4.3	6.8	14.5	18.2	18.6
Representations at $\Gamma$		$\Gamma_4^-$	$\Gamma_1^+$	$\Gamma_5^-, \Gamma_6^+$	$\Gamma_5^+, \Gamma_6^-$	$\Gamma_2^-, \Gamma_3^+$	$\Gamma_1^+, \Gamma_4^-$			
Secondary emission peaks										
			$E_{vac}$	2	3	4	5			
	GaSe		6.0	6.7	7.9	10.2				
	GaS		6.5	7.0	8.0	9.2	10.8			

<sup>a</sup>Weak shoulder only observed for certain angles of photoemission.

minations of the average stacking sequence (e.g., whether  $\beta$ ,  $\epsilon$ , or  $\gamma$ ) are not necessarily relevant to the structure exposed on cleavage because of the possible presence of stacking faults (or their creation during cleavage) close to the surface. Accordingly, comparison between the calculated bands for GaSe and the spectra must be made essentially in the spirit of a two-dimensional approximation, bearing in mind the detailed three-dimensional layer-layer interaction effects only in so far as they may affect specific bands. Furthermore, surface relaxation may be expected to alter the magnitude of such interactions invalidating a too detailed interpretation in terms of layer-layer splitting of bands.

#### B. Final-state and matrix-element weighting

Although in any photoemission experiment, the analyzer may be regarded as picking out a specific initial state, the measured intensity in the photoelectron energy distribution is weighted both by the momentum matrix elements for the optical transition, and by the function representing the joint density of initial and final states (which conserve energy in the transition). The resulting spectra do not, therefore, necessarily reflect the simple initial (i.e., valence-band) density of states. The fluctuations in relative intensity at different photon energies of features in the uppermost band of GaSe may, in principle, derive from either or both of these effects. But, if the valence band comprises only states of  $p$  character, it is difficult to account for these observations in terms of matrix-element variations, since the  $4p$  wave functions of both Ga and Se should have very simi-

lar photoelectric cross sections (in contrast to the marked difference in  $s$  and  $p$  cross sections, which result in negligible  $s$ -state contributions to uv excited photoemission). Only if significant  $d$  character were introduced into the band, would such variations be anticipated on this basis. For GaS, of course, there would be some differences in the cross-section behavior of the Ga  $4p$  and the S  $3p$  states; however, the general form of the intensity fluctuations is similar in both the compounds suggesting similar origins for the effects in both cases.

It would appear, therefore, that for He I and Ne I photons the details in the energy distributions are sensitive to the form of the joint density of states possibly as a result of Se  $4d$  character in the conduction band. However, the spectra for the He II and Mg  $K\alpha$  photons show similar weighting suggesting only a slowly varying density of final states above 30 eV or so; for the purposes of interpretation the He II spectra are thus assumed to be representative of the initial density of states. This proposal takes no account of any possible angular dependence in the photoemitted energy distribution which, as can be seen in the He I spectra in Fig. 6, may be quite marked. Again at the He II energy the angular aperture in the present spectrometer slit system is sufficient to sample wavevector components throughout the first Brillouin zone, so that an average density-of-states comparison is appropriate at this photon energy. At the lower photon energies (Ne I and He I), however, the angular dispersion of photoelectrons from states within the first zone is greater so that the angular selectivity of the slit system becomes more important.

### C. Photoemission threshold and optical energy gap

Experimentally, it is convenient to refer the binding energies of features in the photoemission spectra to the "instrumental" Fermi level. If no macroscopic electric fields exist across the sample, this data should still be valid as a zero of energy at the sample surface so that a photoemission threshold noncoincident with  $E_F$  may be taken as a good criterion of semiconducting behavior. The possibility of band bending at the surface, however, means that the precise relationship between conduction and valence-band edges, and  $E_F$  may differ between the bulk and the surface, particularly under uv or x-ray excitation. In the present investigation, the threshold energy  $E_{vb}$  for both GaS and GaSe is considerably less than the magnitude of the indirect gap (Table I), suggesting that the Fermi level under these experimental conditions is still located in the middle of the forbidden gap. However, as no attempt was made to characterize these crystals as *n*- or *p*-type, we cannot discount the possibility of band bending and accordingly give in Table I the binding-energy values with respect to the band edge  $E_{vb}$ . We only note that the observation of sharp structure in the measured energy distributions suggests that any band bending must occur over a depth which is very much greater than the hot-electron scattering length at uv photon energies as has already been pointed out by McFeeley *et al.*<sup>9</sup> for other semiconducting compounds.

### D. Interpretation of the energy distributions

It is evident from the experimental results that the photoemission spectra exhibit structure from a number of bonding and nonbonding valence bands, as well as giving some information on conduction-band states (from the secondary emission curves). In order to facilitate discussion of these features, which are complicated in the experimental spectra by effects owing to overlap between peaks excited by photons at different energies, we have replotted in Fig. 8 a composite diagram of the measured density of states in GaSe. Thus the states *a*, *b*, *c*, *d*, *e*, and *f* excited by He II photons are followed by the chalcogen *s* band excited by Mg  $K\alpha$ , and the Ga  $3d$  core state (with respect to its correct binding energy relative to the band edge  $E_{vb}$ ) excited by He II $\beta$  photons. The structure interpreted previously as owing to secondary electron emission is plotted according to its energy above the band edge. For comparison, Fig. 8 also reproduces the pseudopotential energy bands calculated by Schluter<sup>5</sup> together with the valence-band density of states derived from this scheme by Baldereschi *et al.*<sup>10</sup> We will discuss the origins of the various photoemission bands separately starting with the

nonbonding *d* and *s* bands.

#### 1. Gallium 3*d* states

Excitation of the Ga  $3d$  core levels is observed at 18.85 and 19.20 eV below  $E_{vb}$  for both the sulphide and the selenide, the  $3d_{5/2}$ - $3d_{3/2}$  spin-orbit splitting being  $0.35 \pm 0.05$  eV in both cases; precise estimates of this splitting are complicated by linewidth effects, but a simple graphical curve synthesis suggests that the true spin-orbit splitting is about 0.1 eV larger than this in closer agreement with the value of 0.45 eV determined by Thiry *et al.*<sup>7</sup> in synchrotron absorption measurements. These authors also determine a  $3d_{5/2}$  binding energy relative to  $E_{vb}$  as 18.6 eV, again in fair agreement with the present measurements.

#### 2. Chalcogen *s* band

The outermost electronic configurations of the chalcogen and metal atoms are  $s^2 p^4$  and  $s^2 p^1$ , respectively; whilst the metal *s* and *p* states may mix and participate in the bonding, the four *s* electrons from the two chalcogen atoms per formula unit form a band much deeper in energy. From Schluter's calculation for  $\beta$ -GaSe and the density of

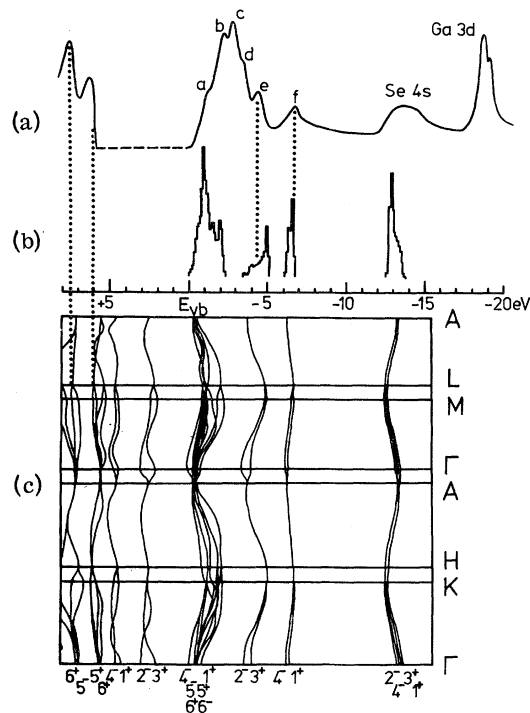


FIG. 8. Composite density of states: (a) for GaSe with secondary emission peaks and in correct position above  $E_{vb}$ , the He II valence band, the Se  $4s$  band excited with Mg  $K\alpha$ , and Ga  $3d$  excited with He II $\beta$ . This is compared with (b) density of states derived by Baldereschi *et al.* (Ref. 10) from (c) the pseudopotential-energy-band scheme of Schluter (Ref. 5).

states derived from this<sup>10</sup> (see Fig. 8), we expect this *s* band to lie at about 13 eV below  $E_{vb}$ , in close agreement with the broad band observed at these energies with Mg  $K\alpha$  x radiation. This *s* band is entirely absent in the He II spectrum as can be seen from the completely flat background in this region in Fig. 2; a similar absence of *s* states is found in the high-energy uv energy distributions from the transition metal dichalcogenides,<sup>11</sup> whereas XPS studies of the same compounds<sup>12</sup> reveal prominent *s* states below the main valence band. Neglecting final-state weighting, as discussed above, the absence of *s* states in the spectra for both GaS and GaSe must, therefore, be explained on the basis of the relative photoelectric cross sections for *s*, *p*, and *d* states at different photon energies.<sup>13</sup> It is interesting to note that the intensity of the Ga 3*d* core level relative to that of the uppermost *p*-like valence band is similar at 48.4 eV (19:1) and at 1253.6 eV (15:1), suggesting similar *p* and *d* cross sections for x rays and these higher-energy uv photons. For He II (40.8 eV) the Ga-3*d*: valence-band ratio is considerably smaller (4:1), amply illustrating the marked dependence on photon energy of the cross sections in the 0–50-eV energy range.

The *s* band also occurs in GaS at about 13.5 eV (with Mg  $K\alpha$ ); in both the sulphide and the selenide, the bandwidth ( $\sim 2$  eV) even allowing for instrumental resolution ( $< 1$  eV) is larger than expected, and contrasts with the narrow 3*d* linewidth for the Ga at similar binding energies. Similar *s* bandwidths are observed in the transition-metal dichalcogenides,<sup>12</sup> but it is not entirely clear in either case whether the photoemission measurements reflect the true bandwidth or whether lifetime effects contribute to the observed broadening.

### 3. Ga-Ga bonding and antibonding bands

The two pairs of bands centered near 4.5 and 6.5 eV in Schluter's calculations exhibit antibonding and bonding character with respect to the Ga  $p_x$  wave functions. Bands *e* and *f* in the photoemission spectra for GaSe, which occur at 4.2 and 6.6 eV, respectively, always scale with the same relative intensity ratio irrespective of photon energy, and may be interpreted in terms of these Ga  $p_x$ -like bands. It should be noted that the peak in the calculated density of states for band *e* appears at the bottom of the band only as a result of its flatness along *KH* and *ML*. However, it is likely that the true shape of this band is somewhat different from that shown in Fig. 8 as a result of the considerable overlap with the upper valence band revealed in the photoemission spectra. Nor can it be certain which states (i. e., wave vectors) contribute most significantly to the present measurements as a consequence of crystal orientation

relative to the analyzer entrance slit. We therefore take the peaks in the measured He II density of states (for which we expect considerable angular averaging as outlined above), to be more characteristic of the centers of gravity of bands, and in this sense there is fair agreement between the measured and calculated band positions for *e* and *f*.

It is interesting to note in the comparison of GaS with GaSe (Figs. 2, 5, and 7; Table I) that this pair of bands maintains the same separation in both cases (2.4 eV) although appearing at higher-binding energy relative to  $E_{vb}$  in the sulphide. At first sight, this result is somewhat surprising, since it can be argued that the increase in forbidden gap in the sulphide relative to the selenide reflects a change in the Ga-Ga wave-function overlap. The lowest conduction band in the calculations for  $\beta$ -GaSe, in fact, shows strong antibonding character between the Ga atoms (as well as between Ga and Se atoms) and its position (and hence the magnitude of the gap) may, therefore, be very sensitive to changes in the Ga positions. Thus as band *e* also exhibits antibonding character with respect to the Ga atoms, it could be expected that as the energy gap increases, so the splitting between bands *e* and *f* should increase, contrary to observation.

However, this apparent anomaly is resolved when we consider the nature of the Ga-Se bonding within the various bands. For band *e*, some bonding charge builds up between the Ga and the Se, in contrast to the lowest conduction band, which is antibonding with respect to Ga-Se overlap. That both bands *e* and *f* increase in binding energy in the sulphide we therefore interpret as indicative of a strengthening of both the Ga-Ga and the Ga-chalcogen bonds in the sulphide relative to the selenide.

### 4. $p_x$ - $p_y$ bands

The uppermost valence states in Schluter's band scheme comprise two groups of bands, those based largely on the chalcogen  $p_x - p_y$  wave functions (containing 16 electrons in the  $\beta$  structure), and the pair of bands with the same symmetries as *e* and *f* based on Ga and the chalcogen  $p_x$  states (containing 4 electrons). It is evident that the calculated overall bandwidth of these upper valence levels is too narrow when compared with the photoemission spectrum in Fig. 8; the considerable overlap with band *e* contrasts with the nearly zero measured density of states between bands *e* and *f*. If we assume that at He II energies, the spectra reflect a reasonable approximation to a one-electron band picture, then it would appear either that the width of the individual bands has been underestimated in the calculations, or that the degree of overlap between the two sets of bands ( $\Gamma_1^+ \Gamma_4^-$  and  $\Gamma_5^+ \Gamma_6^-$  and  $\Gamma_6^+ \Gamma_5^-$ ) has been overestimated, the

center of the latter set of bands being placed at too low a binding energy below  $E_F$ . In discussing these two possible explanations of the discrepancy it is useful once again to compare the results for GaS with those for GaSe, where it was noted previously that the bands  $c$ ,  $d$ ,  $e$ , and  $f$  all appear at higher binding energy relative to  $E_{vb}$  in the sulphide. This leaves bands  $a$  and  $b$  much more clearly split from the remaining states, as is evident at all photon energies in the comparison of Figs. 2 and 5. It has been argued previously that the states  $e$  and  $f$ , which may be identified with the Ga-Ga bonding-antibonding pair, are lowered in energy in the sulphide as a result of increased Ga-Ga and Ga-S interactions. The upper group of  $p_x-p_y$  based states, however, provides the main stability in the Ga-chalcogen bond and would, therefore, also be expected at a higher binding energy in the sulphide than in the selenide, thereby leading to an identification of peaks  $c$  and  $d$  with these  $p_x-p_y$  based bands. In GaSe, this places these bands some 2 eV or so lower than in the calculated scheme leading to some overlap with band  $e$ , which is the Ga-Ga antibonding band ( $\Gamma_2^- \Gamma_3^x$ ).

#### 5. Uppermost valence band ( $p_z$ )

The remaining conclusion to be drawn from the above argument is that bands  $a$  and  $b$  should be identified with the uppermost valence-band pair ( $\Gamma_1^+ \Gamma_4^-$ ). As has been shown by Schluter<sup>5</sup> for GaSe this pair of bands shows some Ga-Ga bonding character. However, little or no bonding charge is built up between the Ga and chalcogen atoms, while a predominant  $p_z$ -like charge builds up on the latter. The extension of this  $p_z$  charge towards neighboring layers results in the splitting of about 1 eV into states with  $\Gamma_1^+$  and  $\Gamma_4^-$  symmetries. This pair of bands may, therefore, be viewed as largely nonbonding, and would not be expected to move to higher binding energy following increased Ga-chalcogen or Ga-Ga interaction in the sulphide. The agreement between the calculated splitting ( $\Gamma_1^+ - \Gamma_4^-$  is 0.7 eV), and the measured splitting of bands  $a$  and  $b$  (1.0 eV for both GaSe and GaS) does indeed suggest a possible identification with the  $\Gamma_1^+ \Gamma_4^-$  pair. However, the fluctuation in relative intensity of  $a$  and  $b$  with photon energy and with angular variation, which might not be anticipated for states of such similar character, precludes too close a comparison; the most direct evidence for  $p_z$  character in this band pair remains their detachment from the other bands in the sulphide relative to the selenide.

#### 6. Conduction-band states and secondary electron emission

Thus far we have taken account only of peaks in the energy distributions deriving from elastically emitted photoelectrons. The emergent photoelec-

tron may, however, be inelastically scattered via screened Coulomb interactions with the other valence electrons, resulting in electron-hole pair creation. Either or both of these electrons (i. e., the scattered photoelectron or the electron in the created pair) may be scattered into states above the vacuum level, producing a contribution to the measured energy distribution spectrum. Kane<sup>14</sup> has shown that such features in the spectrum should then be characteristic of structure in the one-electron conduction-band density of states. If peaks 2 and 3 in the He I and Ne I spectra, whose final-state energies above the band edge were shown to be independent of photon energy, are so interpreted, the agreement between observed and calculated conduction-band positions for GaSe is close as is seen in Fig. 8. Thus the vacuum level at +6.0 eV above  $E_{vb}$  lies within the  $\Gamma_5^+ \Gamma_6^-$  pair of conduction bands, which give rise to peak 2 in the secondary emission spectrum. Peak 3 then arises from excitation into the  $\Gamma_5^+ \Gamma_6^+$  bands. The third weak maximum 4 in the He I spectrum corresponds to the next highest conduction band. The energies of  $E_{vac}$ , 2, and 3 at 6.0, 6.7, and 7.9 eV, respectively, agree closely with the values of 6.2, 6.8, and 7.6 eV, respectively, determined from final states in low-energy photoemission by Thiry *et al.*<sup>7</sup> For GaS the vacuum level appears at 6.5 eV above  $E_{vb}$  so that in the absence of any band bending a work function of  $5.1 \pm 0.5$  eV would be predicted for both materials.

## V. CONCLUSIONS

Photoelectron energy distributions for the layer crystals GaSe and GaS recorded at ultraviolet photon energies show much sharp structure in the valence-band region. Both are found to exhibit behavior consistent with semiconducting properties with similar work functions. Comparison with XPS data has facilitated an accurate determination of the binding energies of the spin-orbit-split Ga 3d core levels, and the chalcogen  $s$  band has been located. The absence of the latter in the uv spectra is attributed to the low cross section for  $s$  states relative to  $p$  and  $d$  states at low photon energies. Whilst final-state modulation may contribute to the relative weighting of structure at lower photon energies (He I and Ne I), spectra recorded at the He II energies are found to reflect to a large degree the valence-band density of states weighted by matrix elements for photoexcitation. Accordingly the measured density of states for GaSe has been compared with that computed from a pseudopotential energy-band calculation, and assisted by a comparison between spectra for GaSe and GaS the possible nature of each measured valence-band feature has been discussed.



Some adjustment in the relative positions of the calculated energy bands is found to be necessary, but otherwise the overall agreement with the present results is good. The energies of structure in the secondary electron-energy distributions are also shown to correlate with features in the conduction-band density of states.

#### VI. ACKNOWLEDGMENTS

We thank F. Levy (EPF, Lausanne) for the supply of the single crystals for this work, A. Baldereschi and M. Matschke for communication of their unpublished densities-of-states calculations, and the Science Research Council for a grant to this laboratory.

\*Present address: Dept. of Chemistry, University of British Columbia, Vancouver B. C., Canada.

†Present address: VG Scientific Ltd., East Grinstead, Sussex, England.

<sup>1</sup>Z. S. Basinski, D. B. Dove, and E. Mooser, *Helv. Phys. Acta* **34**, 373 (1961).

<sup>2</sup>F. Aulich, J. L. Brebner, and E. Mooser, *Phys. Status Solidi* **31**, 129 (1969).

<sup>3</sup>F. Bassani and G. Pastori, *Nuovo Cimento B* **50**, 95 (1967).

<sup>4</sup>E. Mooser, I. Ch. Schlüter, and M. Schlüter, *J. Phys. Chem. Solids* **35**, 1269 (1974).

<sup>5</sup>M. Schlüter, *Nuovo Cimento B* **13**, 313 (1973).

<sup>6</sup>J. M. Thomas, I. Adams, R. H. Williams, and M. Barber, *J. Chem. Soc.* (unpublished); *Trans. Faraday Soc.* **68**, 755 (1972).

<sup>7</sup>P. Thiry, R. Pincheaux, D. Dagneaux, and Y. Petroff,

in *Proceedings of the Twelfth International Conference on the Physics of Semiconductors*, edited by M. H. Pilkhun (Teubner, Stuttgart, 1974), p. 1324.

<sup>8</sup>R. H. Williams, G. P. Williams, C. Norris, M. R. Howells, and I. H. Munro, *J. Phys. C* **7**, L29 (1974).

<sup>9</sup>F. R. Mcfeely, S. P. Kowalczyk, L. Ley, R. G. Cavell, R. A. Pollak, and D. A. Shirley, *Phys. Rev. B* **9**, 5628 (1974).

<sup>10</sup>A. Baldereschi and M. Matschke (private communication).

<sup>11</sup>F. R. Shepherd and P. M. Williams, *J. Phys. C* **7**, 4416 (1974); **7**, 4427 (1974).

<sup>12</sup>G. K. Wertheim, F. J. DiSalvo, and D. N. E. Buchanan, *Solid State Commun.* **13**, 1225 (1973).

<sup>13</sup>D. J. Kennedy and S. T. Manson, *Phys. Rev. A* **5**, 227 (1972).

<sup>14</sup>E. O. Kane, *Phys. Rev.* **159**, 624 (1967).